Journal of Engineering Mathematics **31:** 305–318, 1997.

Axisymmetric stagnation-point flow impinging on a transversely oscillating plate with suction

P. D. WEIDMAN and S. MAHALINGAM
Department of Mechanical Engineering, University of Colorado, Boulder, Colorado 80309-0427, U. S. A.

Received 16 October 1995; accepted in revised form 19 March 1996

Key words: exact solution, stagnation flow, unsteady, suction, viscous

Abstract. The viscous fluid motion generated by axisymmetric stagnation-point flow of strain rate a impinging on a flat plate oscillating in its own plane with velocity amplitude U_0 and frequency ω, including uniform suction of strength W_0 is considered. A coordinate decomposition transforms the full Navier-Stokes equations into a *primary* equation describing the steady flow and a *secondary* equation describing the unsteady motion coupled to the primary solution. The solution to the boundary-value problem is governed by two dimensionless groups: the suction parameter $S = W_0/\sqrt{a\nu}$ and the frequency parameter $\Omega = \omega/a$, where ν is the kinematic viscosity. Numerical integrations performed with a Runge-Kutta routine provide an exact solution to the Navier-Stokes equations. Values of the steady shear stress are found to agree with asymptotic results for large values of $|S|$, with $S > 0$ representing suction and $S < 0$ representing blowing. The magnitude and phase of the unsteady shear stress are given over a range of frequencies sufficient to recover analytical asymptotic results at large values of Ω. The unsteady shear stress lags the wall motion by π radians for $\Omega \to 0$ and by $5\pi/4$ radians when $\Omega \to \infty$. Velocity profiles at selected parameter values during a period of plate oscillation are presented and discussed.

1. Introduction

Exact solutions of the Navier-Stokes equations are sometimes found as a "superposition" of fundamental exact solutions that lead, by separation of coordinate variables, to nonlinear coupled ordinary differential equations. Fundamental flows which are readily superposed include the following presented in chronological order of their discovery: uniform shear flow over a flat plate; the flow induced by a plate oscillating in its own plane beneath a quiescent fluid (Stokes [1]); two-dimensional stagnation-point flow (Hiemenz [2]); the flow induced by a disk rotating in its own plane (Karman [3]); flow over a flat plate with uniform normal suction (Griffith and Meredith [4]); three-dimensional stagnation-point flow (Homann [5]); and axisymmetric stagnation flow on a circular cylinder (Wang [6]). The superposition of uniform shear flow and/or stagnation flow on a body oscillating or rotating in its own plane, with or without suction, has led to the determination of further exact solutions to the Navier-Stokes equations. For example, Howarth [7] superposed two-dimensional and three-dimensional stagnation-point flows. Stuart [8], *inter alia*, added uniform suction at the boundary of a rotating disk. Stuart [9] also gave the solution for a fluid oscillating about a nonzero mean flow parallel to a flat plate with uniform suction. Glauert [10] reported on the superposition of stagnation-point flow on a flat plate oscillating in its own plane, and also considered the case where the plate is stationary and the stagnation stream is made to oscillate. Stuart [11] observed that a uniform shear flow aligned with outflowing two-dimensional stagnation-point flow offers an exact solution. Kelly [12] solved the problem of uniform flow along a flat plate with time-dependent suction and included periodic oscillations of the external stream. Gorla [13, 14] superposed axial cylinder translation and oscillation onto Wang's [6] axisymmetric

stagnation flow normal to a cylinder. Wang [15] reported the case of superposing uniform shear flow over an infinite disk rotating in its own plane. Recently, Cunning [16] has calculated an interesting composite boundary-layer structure when stagnation flow normal to a circular cylinder is attended by cylinder rotation and boundary transpiration.

Most exact superposed solutions lead to a linear *secondary* equation coupled to a nonlinear *primary* equation. The superposed flows studied by Howarth [7] and Wang [15] are exceptions in that both the primary and secondary equations are nonlinearly coupled. In this paper the problem of axisymmetric stagnation-point flow acting on a porous flat plate oscillating transversely in its own plane is considered. Thus, three-dimensional stagnation-point flow impinging on a flat plate is forced by two-dimensional plate oscillation and transpiration normal to the plate.

It should be noted that such solutions are both of academic and practical importance. A recent study by Jung, Mangiavacchi, and Akhavan [17] shows that high-frequency spanwise wall oscillations act to suppress turbulence significantly in wall-bounded flows. In such situations it is necessary to calculate the shear stress and fully understand the nature of the laminar flow that precedes the onset to turbulence at higher Reynolds numbers. The present investigation provides an exact solution for one such wall-bounded flow forced by transverse plate oscillations. In §2 the governing equations and numerical solution procedure are presented. Asymptotic results for steady flow with large suction and blowing and a high-frequency analysis for the unsteady flow are given in §3. The primary results are presented in §4 and closing remarks are made in §5.

2. Equations of motion and solution procedure

Cartesian coordinates $\mathbf{x} = (x, y, z)$ with associated unit vectors $(\mathbf{i}, \mathbf{j}, \mathbf{k})$ and corresponding velocity components $\mathbf{u} = (u, v, w)$ are employed. A plate located in the plane $z = 0$ executes a periodic motion $U_0 \mathrm{e}^{i\omega t}$ along the x-axis beneath axisymmetric stagnation-point flow of strain rate a and the transpiration velocity at the plate boundary is $-W_0$. The motion is governed by the equation of continuity

$$\nabla \cdot \mathbf{u} = 0 \tag{1}$$

and the constant-property Navier-Stokes equations

$$\frac{\partial \mathbf{u}}{\partial t} + (\mathbf{u} \cdot \nabla)\mathbf{u} = -\frac{1}{\rho}\nabla p + \nu \nabla^2 \mathbf{u}, \tag{2}$$

in which ∇ is the Nabla operator, ρ is the fluid density, p the pressure, and ν the kinematic viscosity. An inviscid solution of (1) and (2), valid far above the plate, is given by

$$u = ax, \quad v = ay, \quad w = -2az - W_0, \tag{3}$$

$$p = p_0 - \frac{1}{2}\rho a^2 \left[x^2 + y^2 + 4z^2 + 4aW_0 z\right], \tag{4}$$

where p_0 is the stagnation pressure. We may obtain the solution of the viscous problem by decomposing the velocity field into

$$u = axF'(\zeta) + U_0 G(\zeta)\mathrm{e}^{i\omega t}, \tag{5}$$

$$v = ayF'(\zeta), \tag{6}$$

$$w \;=\; -2\sqrt{a\nu}\,F(\zeta) - W_0, \tag{7}$$

$$\zeta \;=\; \sqrt{a/\nu}\,z, \tag{8}$$

$$p \;=\; p_0 - \frac{\rho a^2}{2}\left[x^2 + y^2 + \left(\frac{4\nu}{a}\right)\left(F^2 + F' + SF\right)\right], \tag{9}$$

in which the terms involving $F(\zeta)$ in (5)–(7) comprise the Cartesian similarity form for steady axisymmetric stagnation-point flow. The velocity field satisfies the equation of continuity (1) exactly. Inserting solution form (5)–(9) into the Navier-Stokes equations (2) we find the coupled pair of ordinary differential equations

$$F''' + 2FF'' - F'^{\,2} + SF'' + 1 \;=\; 0, \tag{10}$$

$$G'' + (2F + S)G' - (F' + i\Omega)G \;=\; 0. \tag{11}$$

The boundary conditions are that the tangential velocity shall equal the oscillating wall velocity at $\zeta = 0$, and that the velocity and pressure shall tend to solution (3)–(4) as $\zeta \to \infty$, with a possible displacement effect in the ζ coordinate. Thus we have

$$F(0) \;=\; F'(0) = 0, \quad F'(\zeta \to \infty) \to 1, \tag{12}$$

$$G(0) \;=\; 1, \quad G(\zeta \to \infty) \to 0. \tag{13}$$

The dimensionless wall suction S and the dimensionless frequency Ω governing the solution space are

$$S = \frac{W_0}{\sqrt{a\nu}}, \quad \Omega = \frac{\omega}{a}, \tag{14}$$

and the amplitude of transverse velocity oscillation U_0 is arbitrary. The formulation is exact for values of U_0 and Ω ranging from zero to infinity and for arbitrary positive (negative) values of S corresponding to plate suction (blowing). The case $U_0 = S = 0$ represents the steady axisymmetric stagnation-point flow originally studied by Homann [5]. The limit $\Omega = S = 0$ corresponding to a flat plate moving transversely at uniform speed U_0 beneath axisymmetric stagnation-point flow was studied by Wang [18]. The case $S = 0$ represents a plate undergoing transverse oscillations beneath axisymmetric stagnation-point flow in the absence of suction. In the present work we consider the new exact solutions wherein all three parameters come into play. To work with real variables, we set $G(\zeta) = G_r(\zeta) + iG_i(\zeta)$ in (11) and (13) to obtain

$$G_r'' + (2F + S)G_r' - F'G_r + \Omega G_i \;=\; 0, \tag{15}$$

$$G_i'' + (2F + S)G_i' - F'G_i - \Omega G_r \;=\; 0, \tag{16}$$

and

$$G_r(0) = 1, \quad G_i(0) = 0, \quad G_r(\zeta \to \infty) = 0, \quad G_i(\zeta \to \infty) = 0. \tag{17}$$

Results may be summarized in plots of the steady and unsteady components of wall shear stress as a function of the control parameters. The instantaneous shear stress on the surface of the oscillating plate calculated from the equation

$$\boldsymbol{\tau} = \mu\left[\frac{\partial u}{\partial z}\mathbf{i} + \frac{\partial v}{\partial z}\mathbf{j}\right]_{z=0} \tag{18}$$

may be written as

$$\boldsymbol{\tau} = \rho a^{3/2}\,\nu^{1/2} F''(0)\, r\, \mathbf{e}_r + \rho U_0\,(a\nu)^{1/2}\,|G'(0)|\mathrm{e}^{i(\omega t+\phi)}\,\mathbf{i}, \tag{19}$$

where

$$|G'(0)| = \sqrt{(G_r'(0))^2 + (G_i'(0))^2}, \quad \phi = \tan^{-1}\left\{\frac{G_i'(0)}{G_r'(0)}\right\}. \tag{20}$$

In (19), $\mathbf{e}_r$ is the unit vector aligned radially on the surface of the plate and $r = \sqrt{x^2+y^2}$. Thus, the shear stress is composed of a steady radially-directed component due to the axisymmetric stagnation-point flow and an unsteady component aligned with the direction of plate oscillation.

We obtain a numerical solution of the boundary-value problem (10), (12) and (15)–(17) by using an iterative and adaptive step-size algorithm based on Runge-Kutta methods employing the function NDSolve in Mathematica [19, pp. 108–109. For prescribed values of S and Ω we treat the equations as initial-value problems, using initial guesses for $F''(0), G_r'(0), G_i'(0)$, and integrate to sufficiently large values of ζ. A residual function, the sum of the squares of the mismatch between the resulting and required far-field conditions $(12)_3$ and $(17)_{3,4}$ is minimized to a given accuracy. Calculations were carried out with 16 significant digits and the resulting functions are accurate up to six significant digits. A far-field value of $\zeta = 3.5$ was found sufficient for all $S \geq 0$. When $S \leq 0$, we found integration to $\zeta = -S + \sqrt{S^2 + (3.5)^2}$ to be adequate.

3. Asymptotic analysis

Asymptotic results for steady flow with large suction S and large blowing $|S|$ when $S < 0$ are given in §3.1. The high-frequency behavior of the unsteady flow is presented in §3.2.

3.1. Steady flow: large suction and blowing

The asymptotic behavior of the steady solution for axisymmetric stagnation-point flow at large and small values of the suction parameter S may be obtained for comparison with the numerical solutions when the plate is stationary, *i.e.* when $U_0 = 0$. The results presented here follow the analysis of Pretsch [20] as outlined in Rosenhead [21, pp. 243–252]. For large suction, $F \sim S$ and neglecting $(1 - F'^2)$ in (10) we obtain

$$F''' + SF'' = 0. \tag{21}$$

The solution satisfying boundary conditions (12) is the asymptotic suction profile

$$F(\zeta) \sim \frac{1}{S}\left(\mathrm{e}^{-S\zeta} - 1\right) + \zeta \quad (S \to \infty) \tag{22}$$

with wall-shear stress proportional to

$$F''(0) \sim S \quad (S \to \infty). \tag{23}$$

For large negative values of S corresponding to strong blowing, we set $S = -|S|$ and consider $|S| >> 1$. It is expected that the boundary layer becomes very thick, in which case

viscous effects will be negligible near the wall. Thus, we neglect the highest derivative term in (10) and obtain

$$2FF'' + (1 - F'^2) - |S|F'' = 0. \tag{24}$$

Using the usual substitution for autonomous equations, we readily find the solution satisfying boundary conditions $(12)_{1,2}$ to be

$$F(\zeta) \sim \frac{1}{2|S|}\zeta^2 \quad (S < 0,\ |S| \to \infty) \tag{25}$$

with wall-shear stress proportional to

$$F''(0) \sim \frac{1}{|S|} \quad (S < 0,\ |S| \to \infty). \tag{26}$$

We now use this result to estimate the standoff distance ζ_{st} of the free stagnation point that results from steady blowing. This point occurs along the axis of symmetry where $w = 0$; from (7) that condition is

$$F(\zeta_{\text{st}}) = \frac{1}{2}|S|. \tag{27}$$

When the blowing is large, (25) and (27) give

$$\zeta_{\text{st}} \sim |S| \quad (S < 0,\ |S| \to \infty). \tag{28}$$

The above results provide the asymptotic behavior of steady axisymmetric stagnation-point flow on a plate in the limits of large suction and large blowing. An approximate result for the wall-shear-stress parameter $F''(0)$ may be obtained by the procedure outlined in Appendix A. This result,

$$F''(0) = \frac{1}{2}\left[S + \sqrt{S^2 + \frac{20}{3}}\right], \tag{29}$$

is useful for initiating integrations at intermediate values of the suction parameter where the asymptotic results do not apply.

3.2. UNSTEADY FLOW: HIGH FREQUENCY

When $\Omega >> 1$, we can expect the strong vorticity waves generated in the vicinity of the wall to dominate the steady stagnation-point flow. In that event we may neglect the contributions from F and F' in (11) may be neglected, leaving the constant-coefficient equation

$$G'' + SG' - i\Omega G = 0. \tag{30}$$

The solution satisfying boundary conditions (13) is readily determined to be

$$G(t) = \mathrm{e}^{-(\alpha_r + i\alpha_i)\zeta}, \tag{31}$$

where

$$\alpha_r \;=\; \frac{1}{2}\left[S + \sqrt{\frac{1}{2}\left(\sqrt{S^4+16\Omega^2}+S^2\right)}\right], \tag{32}$$

$$\alpha_i \;=\; \frac{1}{2}\sqrt{\frac{1}{2}\left(\sqrt{S^4+16\Omega^2}-S^2\right)}. \tag{33}$$

The unsteady component of u, denoted herein by $\tilde{u}(\zeta,t)$, calculated as the real part of the unsteady component of (5), is therefore

$$\tilde{u}(\zeta,t) = U_0 \mathrm{e}^{-\alpha_r\zeta}\,\cos(\omega t - \alpha_i\zeta) \quad (\Omega >> 1). \tag{34}$$

Of particular interest for comparison with the numerical calculations to be presented in §4 is the unsteady component of shear stress $\tilde{\tau}$ acting in the direction of plate oscillation, *viz*.,

$$\tilde{\tau} = \mu\frac{\partial\tilde{u}}{\partial z}\Big|_{z=0} = \rho\sqrt{a\nu}\,U_0|\alpha|\cos(\omega t+\pi+\phi) \quad (\Omega >> 1) \tag{35}$$

in which the modulus and phase of α are

$$|\alpha| = \sqrt{\alpha_r^2+\alpha_i^2}, \;\text{ and }\; \phi = \tan^{-1}\left(\frac{\alpha_i}{\alpha_r}\right). \tag{36}$$

Comparison with (19) shows that $|\alpha|$ and ϕ given here are the asymptotic forms for the modulus and phase of $G'(0)$. Two limits of interest may be discerned from the above results. If in addition to high frequency we have $4\Omega >> S^2$, the modulus and phase have the limiting forms

$$|\alpha| \sim \sqrt{\Omega}, \quad \phi \sim \frac{\pi}{4} \quad (4\Omega >> S^2,\ \Omega >> 1). \tag{37}$$

On the other hand, if in addition to high frequency we have $S^2 >> 4\Omega$, the limiting forms are

$$|\alpha| \sim S, \quad \phi \to 0 \quad (S^2 >> 4\Omega,\ \Omega >> 1). \tag{38}$$

In the former case, according to (34)–(36), the wall-shear stress lags the plate motion by $5\pi/4$ radians, while in the latter case the wall-shear stress and plate motion are exactly out of phase.

4. Presentation of results

Before exploring the unsteady solutions, we carried out an integration of the steady stagnation flow with suction and blowing. The results are presented as a parametric plot of $F''(0)$ *versus* S in Figure 1. Also included in the figure are the asymptotic results for large suction (23), large blowing (26), and the approximate solution for $F''(0)$ given by (29). One observes that (29) provides a good representation for the steady shear-stress parameter for $S > -1$, but below this value the approximation becomes increasingly inaccurate. Specifically, the approximate value of $F''(0)$ tends to zero as $5/3|S|$ while the true asymptotic behavior is $1/|S|$.

The steady dimensionless displacement thickness, $\hat{\delta}^* = \sqrt{a/\nu}\,\delta^*$, given by

$$\hat{\delta}^* = \int_0^\infty \left[1 - F'(\zeta)\right]\, d\zeta \tag{39}$$

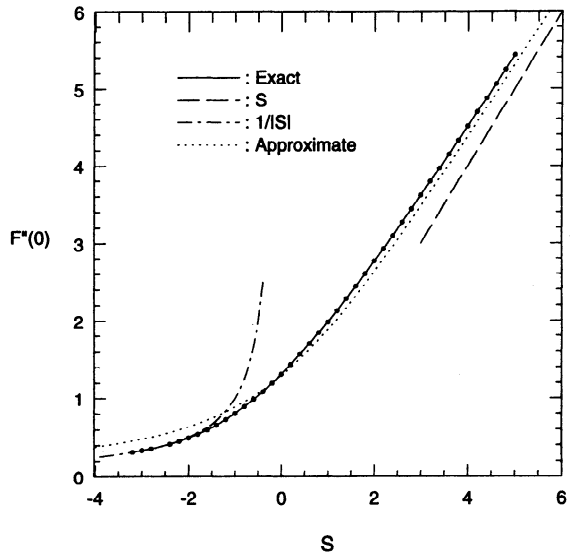

Figure 1. Steady shear-stress parameter $F''(0)$ as a function of the suction parameter S. Solid points are numerical computations, dashed lines represent large suction and blowing asymptotics as noted in the legend, and the dotted curve is the approximate solution given by Equation (29).

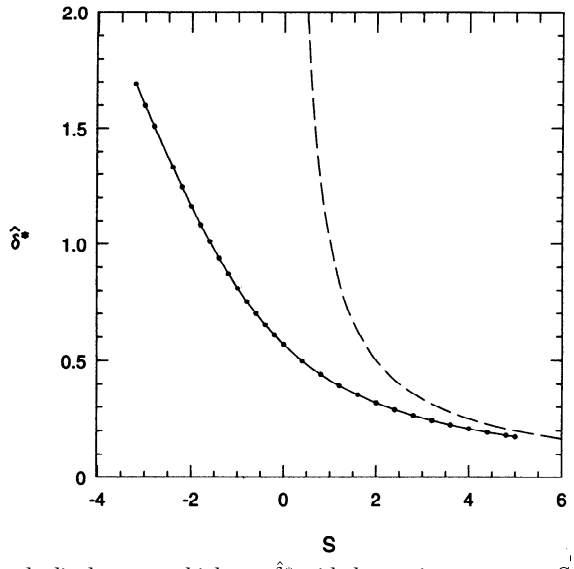

Figure 2. Variation of the steady displacement thickness $\hat{\delta}^*$ with the suction parameter S. Solid points are numerical computations and the dashed curve represents the large suction asymptotics $\hat{\delta}^* \sim 1/S$.

varies markedly with S. Note that δ^* is the dimensional displacement thickness. We may obtain the variation of $\hat{\delta}^*$ at large values of suction by inserting the derivative of (22) into (39), which yields the asymptotic result

$$\hat{\delta}^* \sim \frac{1}{S} \quad (S \to \infty). \tag{40}$$

The large-blowing asymptotic behavior cannot be obtained from (25), since that result is not uniformly valid in ζ. Numerical evaluations of (39) over a range of S are compared with the

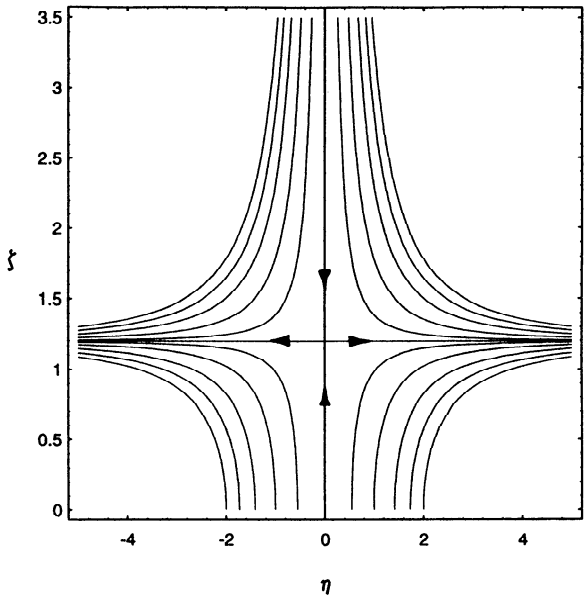

Figure 3. Dimensionless Stokes stream function field $\Psi(\eta, \zeta)$ plotted for $S = -1$ showing the standoff position of the free stagnation point located at $\zeta_{\rm st} \cong 1.20$. The contours correspond to $\Psi = 0,\ \pm 0.15,\ \pm 0.5,\ \pm 1.0,\ \pm 1.5$ and ± 2.0. Arrows indicating the direction of flow appear only on the $\Psi = 0$ contours.

asymptotic result (40) in Figure 2. As expected, the boundary layer becomes progressively thinner with increasing suction and thickens rapidly with blowing.

For steady axisymmetric Homann flow with suction a Stokes stream function $\psi(r, z)$ exists. A dimensionless stream function may be defined as

$$\Psi(\eta, \zeta) = \frac{\psi(\eta, \zeta)}{(\nu^3/a)^{1/2}} = -\eta^2 \left[F(\zeta) + \frac{2}{S} \right], \tag{41}$$

where $\eta = \sqrt{(a/\nu)}\, r$ is the radial coordinate scaled in the same manner as the vertical coordinate. A plot of the streamlines for $S = -1$ in the neighborhood of the free stagnation point presented in Figure 3 shows a standoff distance $\zeta_{\rm st} \cong 1.20$. Numerical determinations of the standoff distance defined by (27) at selected values of S are compared with the large blowing asymptotics for $\zeta_{\rm st}$ given by (28) in Figure 4.

Numerical integration of (15)–(17) governing the unsteady behavior of the motion becomes increasingly difficult for large values of Ω and large negative values of S. This is due to the fact that the thickness of the unsteady boundary layer embedded within the steady boundary layer becomes small relative to $\hat{\delta}^*$, making the equations increasingly stiff. Nevertheless, we have carried out integrations over a wide range of dimensionless frequencies $0 < \Omega < 1000$ for selected values of S in the range $-2 < S < 2$.

The unsteady numerical results may be summarized in a plot of the magnitude and phase of the shear stress as functions of Ω with parameter S. Figure 5a exhibits the variations of $|G'(0)|$ with frequency in the low-frequency range $0 < \Omega < 14$ for the selected values of S. In Figure 5b the corresponding variations of phase ϕ with frequency are shown. Note that for blowing the phase overshoots its asymptotic value, approaching $\pi/4$ from above. The high-frequency behavior of these quantities plotted in semi-log form for frequencies up to $\Omega = 1000$ are given in Figures 6a,b which also include, plotted as dashed lines, the asymptotic behaviors

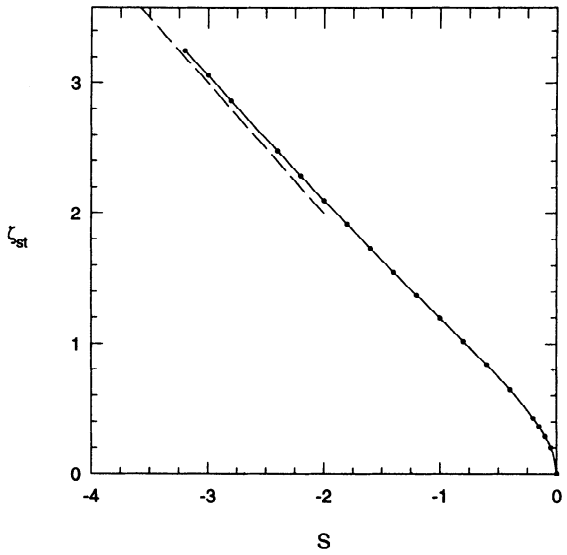

Figure 4. Variation of the standoff distance ζ_{st} of the free stagnation point as a function of blowing strength $-S$. Solid points are numerical computations and the dashed curve represents the large blowing asymptotics $\zeta_{st} \sim |S|$.

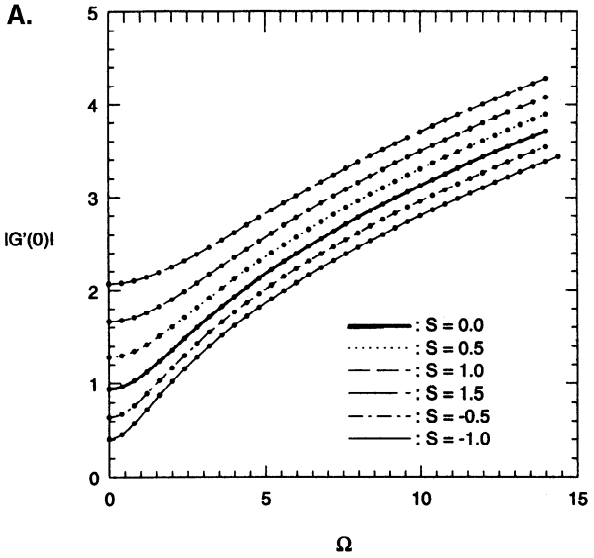

Figure 5a. Low-frequency ~~variation of the unsteady shear-stress parameter $|G'(0)|$ for s~~elected values of S.

of $|G'(0)|$ and ϕ according to (32), (33) and (36). It may be observed that the numerical results tend toward the S-independent asymptotic limits given in (37) as $\Omega \to \infty$. In particular, the phase ϕ, at each value of S, tends asymptotically toward the constant value $\pi/4$, in agreement with other oscillatory problems of this type [9, 10, 12]. Note in Figure 6b that the convergence of ϕ toward its final asymptotic value is very slow.

In the case of suction, the instantaneous position of zero wall-shear stress implies the instantaneous position $\mathbf{x}_s$ of the stagnation point. Setting $\tau = 0$ in (19), and taking the real part, we obtain $y_s = 0$ and

$$x_s = -\left(\frac{U_0\,|G'(0)|}{aF''(0)}\right)\cos(\omega t + \phi). \tag{42}$$

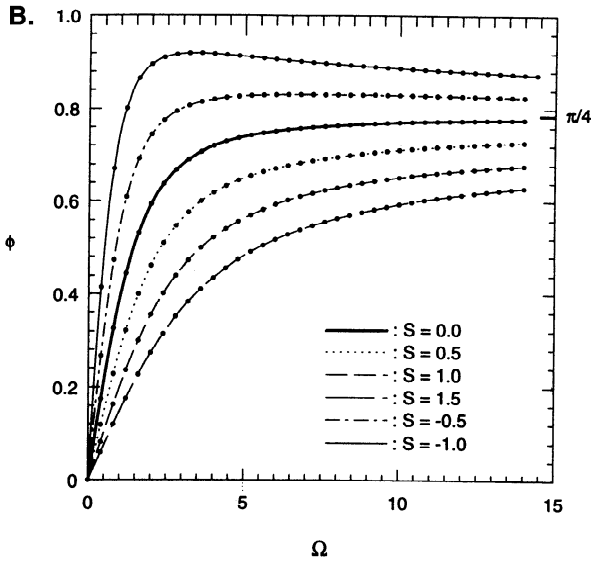

Figure 5b. Low-frequency variation of the phase ϕ of unsteady shear-stress for selected values of S.

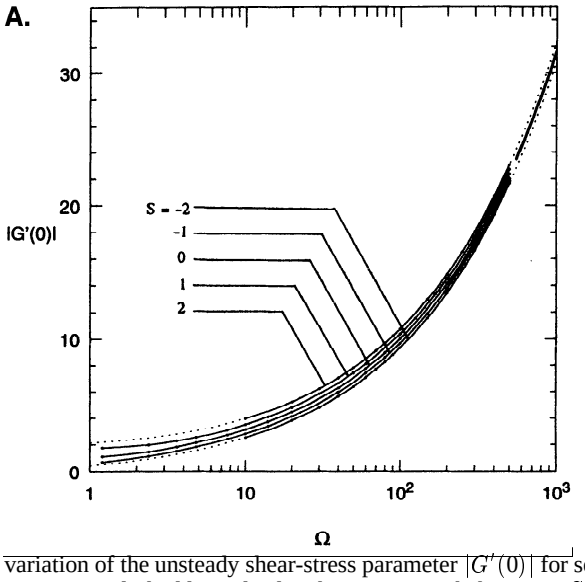

Figure 6a. High-frequency variation of the unsteady shear-stress parameter $|G'(0)|$ for selected values of S. Solid points are the numerical computations, dashed lines display the asymptotic behavior at $S = \pm 2$, and the bold solid line represents the S-independent asymptotic limit.

When the plate moves steadily at speed U_0 for which $\omega = \phi = 0$, we find $x_s = 0.715531\, U_0/a$ in agreement with Wang [18].

We render the velocity component (5) along the direction of plate oscillation dimensionless by dividing through by U_0. Taking the real part we find

$$\frac{u}{U_0} = \hat{u}(\zeta) + \tilde{u}(\zeta, t) = \left(\frac{ax}{U_0}\right) F'(\zeta) + \left[G_r(\zeta)\cos\omega t - G_i(\zeta)\sin\omega t\right], \tag{43}$$

where the steady component $\hat{u}(\zeta)$ and the unsteady component $\tilde{u}(\zeta, t)$ are implicitly defined in the equation. A plot of $\tilde{u}(\zeta, t)$ *versus* ζ over a complete oscillation period at $\pi/4$ increments of ωt is shown in Figure 7 for the selected parameter values $S = 0$ and $\Omega = 10$. Although

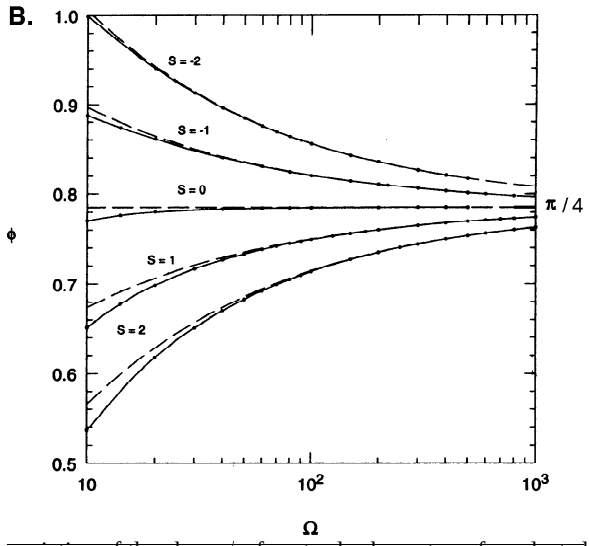

Figure 6b. High-frequency variation of the phase ϕ of unsteady shear stress for selected values of S. Solid points are the numerical computations, dashed lines display the asymptotic behavior at each S, and the bold solid line represents the S-independent asymptotic limit $\phi = \pi/4$.

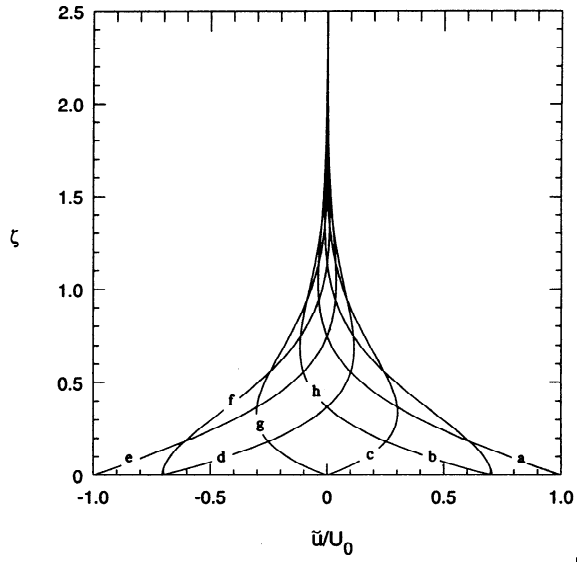

Figure 7. Normalized $\tilde{u}(\zeta, t)/U_0$ unsteady velocity profiles along the direction of plate oscillation at $S = 0$ and $\Omega = 10$ displayed at equal time increments during one period of plate oscillation: (a) $\omega t = 0$, (b) $\pi/4$, (c) $\pi/2$, (d) $3\pi/4$, (e) π, (f) $5\pi/4$, (g) $3\pi/2$, (h) $7\pi/4$.

the variation of $\tilde{u}$ with ζ is smooth, note that it is not monotonic. At higher frequencies the profiles are similar, only compressed toward the wall, indicating that less of the outer flow field is affected by the plate oscillation. For increasing (decreasing) values of the suction parameter S, similar compression (expansion) of the velocity profiles is observed. Profiles of the total velocity u/U_0 along the direction of plate oscillation over one oscillation period at the location $(x, y) = (U_0/a,\ 0)$ are shown in Figure 8 for $S = -1$ and $\Omega = 10$. Note that for $\omega t \geq \pi/2$ when the plate is moving in the negative x-direction, the fluid adjacent to the

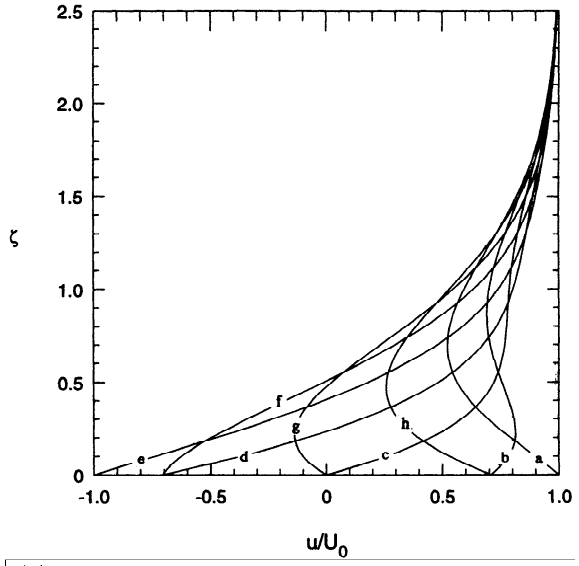

Figure 8. Normalized $u(\zeta, t)/U_0$ total velocity profiles along the direction of plate oscillation at $S = -1$ and $\Omega = 10$ displayed at equal time increments during one period of plate oscillation: $(x, y) = (U_0/a, 0)$, (a) $\omega t = 0$, (b) $\pi/4$, (c) $\pi/2$, (d) $3\pi/4$, (e) π, (f) $5\pi/4$, (g) $3\pi/2$, (h) $7\pi/4$.

plate moves in unison with it, whereas the fluid in regions distant from the plate moves in the positive x-direction, indicating the presence of reversed flow.

5. Summary and conclusion

The problem of axisymmetric stagnation-point flow impinging on a flat plate oscillating in its own plane with suction and blowing has been solved by reduction of the Navier-Stokes equations to a set of coupled ordinary differential equations and subsequent numerical integration. Numerical solutions are given over a range of dimensionless frequencies $0 < \Omega < 1000$ and dimensionless suction strengths $-2 < S < 2$. The numerical calculations clearly tend to the asymptotic expressions for the steady shear-stress parameter $F''(0)$ as $|S| \to \infty$, both in the limit of large suction ($S > 0$) and in the limit of large blowing ($S < 0$), although the convergence in the former is much slower than in the latter. With large blowing the position of the free stagnation point in the steady flow problem is observed to approach the asymptotic prediction $\zeta_{\rm st} \sim |S|$.

The magnitude $|G'(0)|$ and phase ϕ of the unsteady shear stress induced by the oscillating wall have been computed over the range of suction and blowing $-2 < S < 2$. The low-frequency variations of these quantities evolve to the high-frequency asymptotic behaviors determined by analysis. We find that the phase lag $(\pi + \phi)$ between the wall-shear stress and the oscillating plate tends to the constant value $5\pi/4$ at high frequencies, a result anticipated from the original work of Lighthill [22] and Stuart [9]. The numerical results confirm that the high-frequency asymptotics provide an accurate description of the flow for all $\Omega > 100$, at least for the range of transpirations covered in this study.

Appendix

A. An approximation for the steady shear-stress parameter

In integrating the steady equation for $F(\zeta)$ we must iterate on $F''(0)$ to satisfy the far-field boundary condition $(12)_3$ as $\zeta \to \infty$. Estimates for this initial value useful in carrying out the numerical integrations may be obtained by the following procedure. It is convenient to introduce the suction parameter S into the boundary condition by writing, in lieu of (7),

$$w = -2\sqrt{a\nu}\, f(\zeta), \tag{44}$$

which gives rise to the boundary-value problem

$$f''' + 2ff'' + (1 - f'^2) = 0, \tag{45}$$

$$f(0) = S/2, \quad f'(0) = 0, \quad f'(\zeta \to \infty) = 1. \tag{46}$$

In this formulation we see that the suction parameter appears in the boundary conditions rather than in the differential equation itself. We introduce a stretching parameter α through the affine transformation

$$\xi = \alpha\zeta, \quad g = \alpha f \tag{47}$$

to obtain the modified boundary-value problem

$$\alpha^2 g''' + 2gg'' + (1 - g'^2) = 0, \tag{48}$$

$$g(0) = \frac{\alpha S}{2}, \quad g'(0) = 0, \quad g'(\xi \to \infty) = 1, \tag{49}$$

where a prime now denotes differentiation with respect to ξ. The asymptotic suction profile solution to this equation is given by

$$g(\xi) = \xi - 1 + \mathrm{e}^{-\xi} + \frac{\alpha S}{2} \tag{50}$$

and we aim to minimize the square of the residual function obtained by inserting (50) into the governing equation (45). The residual is readily calculated to be

$$R(\xi, \alpha) = \mathrm{e}^{-2\xi} + [2\xi + \alpha(S - \alpha)]\, \mathrm{e}^{-\xi} \tag{51}$$

and, integrating its square over the fluid domain, we arrive at

$$Q(\alpha) = \int_0^\infty R^2(\xi, \alpha)\, d\xi = \frac{1}{2}\alpha^2(S - \alpha)^2 + \frac{5}{3}\alpha(S - \alpha) + \frac{53}{36}. \tag{52}$$

Finally, we minimize $Q(\alpha)$ with respect to α to obtain a cubic equation for α. The relevant root is

$$\alpha = \frac{1}{2}\left[S + \sqrt{S^2 + \frac{20}{3}}\right] \tag{53}$$

and from (47) and (50) we find $F''(0) = \alpha$. This is the result reported as Equation (29) in the main text.

References

1. G.G. Stokes, On the effect of the internal friction of fluids on the motion of pendulums. *Transactions of the Cambridge Philosophical Society* 9 (1851) Part II, 8-106.

2. K. Hiemenz, Die Grenzschicht an einem in den gleichförmingen Flussigkeitsstrom eingetauchten geraden Kreiszylinder. *Dinglers Polytechnisches Journal* 326 (1911) 321-410.
3. T. von Kármán, Über laminare und turbulente Reibung. *Zeitschrift für angewandte Mathematik und Mechanik* 1 (1921) 233-252.
4. A. A. Griffith and F. W. Meredith, The possible improvement in aircraft performance due to the use of boundary layer suction. Royal Aircraft Establishment Report No. E 3501 (1936) 12pp.
5. F. Homann, Der Einfluss grosser Zähighkeit bei der Strömung um den Zylinder und um die Kugel. *Zeitschrift fur angewandte Mathematik und Mechanik* 16 (1936) 153-164.
6. C.-Y. Wang, Axisymmetric stagnation flow on a cylinder. *Quarterly of Applied Mathematics* 32 (1974) 207-213.
7. L. Howarth, The boundary layer in three-dimensional flow. Part II: The flow near a stagnation point. *Philosophical Magazine* 42 (1951) 1433-1440.
8. J. T. Stuart, On the effects of uniform suction on the steady flow due to a rotating disk. *Quarterly Journal of Mechanics and Applied Mathematics* 7 (1954) 446-457.
9. J. T. Stuart, A solution of the Navier-Stokes and energy equations illustrating the response of skin friction and temperature of an infinite plate thermometer to fluctuations in the stream velocity. *Proceedings of the Royal Society* London A 231 (1955) 116-130.
10. M. B. Glauert, The laminar boundary layer on oscillating plates and cylinders. *Journal of Fluid Mechanics* 1 (1956) 97-110.
11. J. T. Stuart, The viscous flow near a stagnation point when the external flow has uniform vorticity. *Journal of Aero/Space Science* 26 (1959) 124-125.
12. R. E. Kelly, The flow of a viscous fluid past a wall of infinite extent with time-dependent suction. *Quarterly Journal of Mechanics and Applied Mathematics* 18 (1965) 287-298.
13. R. S. R. Gorla, Nonsimilar axisymmetric stagnation flow on a moving cylinder. *International Journal of Engineering Science* 16 (1978) 392-400.
14. R. S. R. Gorla, Unsteady viscous flow in the vicinity of an axisymmetric stagnation point on a circular cylinder. *International Journal of Engineering Science* 17 (1979) 87-93.
15. C.-Y. Wang, Shear flow over a rotating plate. *Applied Scientific Research* 46 (1989) 89-96.
16. G. Cunning, Axisymmetric stagnation point flow on a rotating circular cylinder with uniform transpiration. Masters of Science Thesis, 1995, University of Colorado, Boulder, Colorado, USA.
17. W. L. Jung, N. Mangiavacchi and R. Akhavan, Suppression of turbulence in wall-bounded flows by high-frequency spanwise oscillations. *Physics of Fluids A* 4 (1992) 1605-1607.
18. C.-Y. Wang, Axisymmetric stagnation flow towards a moving plate. *American Institute of Chemical Engineering Journal* 19 (1973) 961 pp.
19. S. Wolfram, *Mathematica: A system for doing mathematics by computer*, 2nd edition. Redwood City: Addison-Wesley (1991) 108-109.
20. J. Pretsch, Über die Stabilität einer Laminarströmung um eine Kugel. *Luftfahrtforschung* 18 (1941) 341-344. (Translated as 'The stability of laminar flow past a sphere', *Technical Memorandum of the National Advisory Committee for Aeronautics*, No. 1017.)
21. L. Rosenhead, *Laminar Boundary Layers*. Oxford: Oxford University Press (1963) 688 pp.
22. M. J. Lighthill, The response of laminar skin friction and heat transfer to fluctuations in the stream velocity. *Proceedings of the Royal Society* London A 224 (1954) 1-23.